JB Journals.ASM.org

# Salinity-Dependent Impacts of ProQ, Prc, and Spr Deficiencies on *Escherichia coli* Cell Structure

**Craig H. Kerr,* Doreen E. Culham, David Marom, Janet M. Wood**

Department of Molecular and Cellular Biology, University of Guelph, Guelph, Ontario, Canada

**ProQ is a cytoplasmic protein with RNA chaperone activities that reside in FinO- and Hfq-like domains. Lesions at *proQ* decrease the level of the osmoregulatory glycine betaine transporter ProP. Lesions at *proQ* eliminated ProQ and Prc, the periplasmic protease encoded by the downstream gene *prc*. They dramatically slowed the growth of *Escherichia coli* populations and altered the morphologies of *E. coli* cells in high-salinity medium. ProQ and Prc deficiencies were associated with different phenotypes. ProQ-deficient bacteria were elongated unless glycine betaine was provided. High-salinity cultures of Prc-deficient bacteria included spherical cells with an enlarged periplasm and an eccentric nucleoid. The nucleoid-containing compartment was bounded by the cytoplasmic membrane and peptidoglycan. This phenotype was not evident in bacteria cultivated at low or moderate salinity, nor was it associated with murein lipoprotein (Lpp) deficiency, and it differed from those elicited by the MreB inhibitor A-22 or the FtsI inhibitor aztreonam at low or high salinity. It was suppressed by deletion of *spr*, which encodes one of three murein hydrolases that are redundantly essential for enlargement of the murein sacculus. Prc deficiency may alter bacterial morphology by impairing control of Spr activity at high salinity. ProQ and Prc deficiencies lowered the ProP activity of bacteria cultivated at moderate salinity by approximately 70% and 30%, respectively, but did not affect other osmoregulatory functions. The effects of ProQ and Prc deficiencies on ProP activity are indirect, reflecting their roles in the maintenance of cell structure.**

Osmotic stress perturbs cell structure, composition, and function (1). Despite retaining their rod-like shape, *Escherichia coli* cells cultivated in high-salinity minimal medium maintain lower hydration, turgor pressure, and growth rate than those cultivated at a lower salinity that is optimal for growth (2). The elastic murein sacculus is believed to buffer effects of osmotically induced water fluxes on cell structure (3). *E. coli* can attenuate osmotically induced dehydration by accumulating small, uncharged, or zwitterionic organic solutes called osmolytes (1, 4, 5). For example, transporter ProP mediates the accumulation of diverse solutes, including proline and glycine betaine, thereby restoring cellular hydration and stimulating bacterial growth in high-salinity media (6, 7).

ProQ is a cytoplasmic protein that binds RNA, facilitating RNA duplexing and strand exchange (8). Previous work showed that *proQ* lesions decreased ProP levels and attenuated ProP activity (the *proQ* transport phenotype). These effects occurred when bacteria expressed *proP* from the chromosome or a plasmid-based $P_{BAD}$ promoter during growth in low- to moderate-salinity media and were reversed by plasmid-based *proQ* expression (8, 9). Here, we show that *proQ* lesions dramatically slow the growth of *E. coli* populations in high-salinity medium and alter the morphologies of *E. coli* cells (the *proQ* growth and morphological phenotypes). They also impair expression of the downstream locus *prc*. Periplasmic protease Prc (also known as Tsp) has been implicated in cell division and protein quality control (10–14).

This report further defines the impacts of *proQ* and *prc* lesions on *E. coli* cell structure, associates ProQ and Prc deficiencies with distinct mutant phenotypes, and shows that *proQ* lesions do not impair osmoregulatory systems other than ProP. These data suggest that the *proQ* transport phenotype reflects more fundamental roles of ProQ and Prc in the maintenance of cell structure.

## MATERIALS AND METHODS

**Bacterial strains and plasmids.** The relevant genotypes and immediate ancestors of the *E. coli* strains and the plasmids used for this study are listed in Tables 1 and 2. The kanamycin (Km) resistance cassettes from Keio collection isolates JW5300-1 (Δ*proQ756*::*kan*) and JW2163 (Δ*spr732*::*kan*) (15) were introduced to strain RM2 by P1 transduction, then deleted as described by Datsenko and Wanner (16) to create deletions in the *proQ* and *spr* loci (Δ*proQ856*::*FRT* and Δ*spr832*::*FRT*, respectively). Transductions were performed with phage P1 *cml clr_100* or P1 *vir* as described by Miller (17).

Routine DNA manipulation, plasmid construction, electrophoresis, and transformation were carried out as described previously (18, 19). Oligonucleotides were purchased from Operon Technologies (Eurofins MWG Operon, Huntsville, AL). PCR was performed as described previously (20). Plasmid pDC77 was created by replacing a fragment of vector pBAD24 (21) flanked by NcoI and HindIII restriction sites with a DNA fragment extending from an NcoI site overlapping the *proQ* initiation codon through a HindIII site adjacent to the *proQ* termination codon (9). Plasmid pCK3 was created by replacing a fragment of vector pBAD33 (21) flanked by SacI and SalI restriction sites with a PCR amplicon obtained using primers prc-1, 5′-GCGAGCTCAGGAGGAAGTGCACATGAACA TGTTTTTTAGGCTTACCG-3′, and prc-2, 5′-GCGTCGACTTACTTGA CGGGAGCGGGT-3′, with chromosomal DNA from *E. coli* MG1655 as

Received 11 July 2013 Accepted 12 January 2014

Published ahead of print 17 January 2014

Address correspondence to Janet M. Wood, jwood@uoguelph.ca.

* Present address: Craig H. Kerr, Department of Biochemistry and Molecular Biology, Life Sciences Institute, University of British Columbia, Vancouver, BC, Canada.

Supplemental material for this article may be found at http://dx.doi.org/10.1128/JB.00827-13.



doi:10.1128/JB.00827-13

**TABLE 1** Origins and relevant genotypes of *E. coli* strains[a]

| Strain | Source strain | Genotype at locus | | | | Reference |
|---|---|---|---|---|---|---|
| | | *proP* | *proQ* | *prc* | *spr* | |
| MG1655 | | *proP*$^+$ | *proQ*$^+$ | *prc*$^+$ | *spr*$^+$ | 70 |
| RM2 | CSH4 | *proP*$^+$ | *proQ*$^+$ | *prc*$^+$ | *spr*$^+$ | 71 |
| WG170 | RM2 | *proP219* | *proQ*$^+$ | *prc*$^+$ | *spr*$^+$ | 45 |
| WG174 | RM2 | *proP*$^+$ | *proQ220*::Tn*5* | *prc*$^+$ | *spr*$^+$ | 45 |
| WG703 | RM2 | *proP*$^+$ | *proQ*$^+$ | Δ*prc3*::*kan* | *spr*$^+$ | 9 |
| WG1072 | RM2 | *proP*$^+$ | Δ*proQ756*::*kan* | *prc*$^+$ | *spr*$^+$ | This study |
| WG1074 | WG170 | *proP219* | *proQ220*::Tn*5* | *prc*$^+$ | *spr*$^+$ | This study |
| WG1119 | RM2 | *proP*$^+$ | Δ*proQ856*::*FRT* | *prc*$^+$ | *spr*$^+$ | This study |
| WG1457 | RM2 | *proP*$^+$ | *proQ*$^+$ | *prc*$^+$ | Δ*spr832*::*FRT* | This study |
| WG1458 | WG1457 | *proP*$^+$ | *proQ*$^+$ | Δ*prc3*::*kan* | Δ*spr832*::*FRT* | This study |

[a] All strains were derived from *E. coli* CSH4 (F$^-$ *trp lacZ rpsL thi*) (73, 74). RM2 is CSH4 Δ*putPA101* (71).

the template. GFPmut2 was carried by plasmid pMGS053 and expressed from a *lac* promoter under the control of LacI carried in *trans* by pREP4 (22). A variant of GFPmut3 that localizes to the periplasm of *E. coli* cells was carried on plasmid pJW1 (23).

**Bacterial cultures.** Bacteria were cultivated in Luria-Bertani (LB) medium (17) or in morpholinopropanesulfonic acid (MOPS) medium (24) with $NH_4Cl$ (9.5 mM) as nitrogen source and glycerol (0.4% [vol/vol]) as carbon source and tryptophan (245 μM) and thiamine (1 mg/ml) to meet auxotrophic requirements. Ampicillin (100 μg/ml), kanamycin (50 μg/ml), and chloramphenicol (30 μg/ml) were added to maintain plasmids. Media osmolalities were adjusted with NaCl and measured as specified by the manufacturer with a vapor pressure osmometer (Wescor, Logan, UT). Cultures were grown at 37°C in a rotary shaker at 200 rpm. Optical densities were monitored with a Bausch and Lomb Spectronic 88 or a Pharmacia Novaspec II spectrometer. A22 (5 μg/ml; Calbiochem) was added during the final subculture to inhibit MreB, and aztreonam (1 μg/ml; Sigma-Aldrich) was added during the final subculture to inhibit penicillin binding protein 3 (PBP3, also known as FtsI).

**Transport assays.** Bacteria were grown in MOPS minimal medium adjusted with NaCl to achieve the desired salinity, and ProP activity was measured using L-[U-$^{14}$C]proline as the substrate (200 μM; 5 Ci/mol), as described before (25). ProU activity was measured in the same way, at an osmolality of 0.75 mol/kg, using [1-$^{14}$C]glycine betaine as the substrate (10 μM; 5 Ci/mol).

**Trehalose assay.** Trehalose accumulation was detected essentially as previously described (26). Bacteria were cultivated in MOPS medium, as for transport assays, without or with 250 mM NaCl. They were harvested from 10 ml of culture (12,096 × *g*, 10 min, room temperature), washed with 1 ml of the same medium lacking the carbon source, and resuspended in 15 μl of 15% trichloroacetic acid (TCA). The suspension was incubated on ice for 10 min, then centrifuged (15,800 × *g*, 10 min, room temperature). Supernatants were spotted on silica gel 60 F254 thin-layer chromatography (TLC) plates (SiliCycle, Quebec City, PQ, Canada). The volume of each extract applied to the plate represented 0.25 μg of cell protein, as determined by analyzing a separate aliquot of each culture in a bicinchoninic acid (BCA) protein assay (27). TLC plates were developed with butanol-ethanol-water (5:3:2) and then charred at 125°C on a hot plate after dipping in sulfuric acid-ethanol (1:4).

**TABLE 2** Plasmids used in this study

| Plasmid | Description | Source |
|---|---|---|
| pCK3 | *prc* in vector pBAD33 (21) | This study |
| pDC77 | *proQ* in vector pBAD24 (21) | 9 |
| pMGS053 | Carries gene for GFPmut2 (72) inserted into vector pQE12 (Qiagen, Inc.) | 22 |
| pJW1 | Carries gene for periplasm-targeted GFPmut2* in vector pASK-IBA3plus (IBA, Göttingen, Germany) | 23 |
| pREP4 | Harbors LacI$^q$ | Qiagen, Inc. |

**Protein assays.** Protein concentrations were determined with the BCA assay (27) with reagents from Pierce (Rockford, IL) according to the manufacturer's instructions and with bovine serum albumin as the standard.

**Microscopy.** Bacteria were cultivated as for transport assays in MOPS medium supplemented with NaCl (25), and samples were prepared for microscopy as previously described (28). Nucleoids were stained with DAPI (4′6-diamidino-2-phenylindole; 50 μg/ml), and membranes were stained with FM4-64 [*N*-(3-triethylammoniumpropyl)-4-(6-(4-(diethylamino)phenyl)hexatrienyl) pyridinium dibromide; 20 μg/ml] as previously described (28). Bacterial viability was tested with the *Bac*Light stain (all stains were from Invitrogen, New London, CN, Canada).

Expression of periplasmic green fluorescent protein (GFP; carried on pJW1) was induced for 45 min by adding anhydrotetracycline (Acros Organics, Geel, Belgium; 15 μg/ml) to the final subculture. After 45 min, expression was stopped by harvesting and resuspending the cells in MOPS medium lacking anhydrotetracycline. The culture was then incubated for a postinduction period of 8 h to attain the desired optical density. Expression of cytoplasmic GFP was not induced.

The peptidoglycan layer was stained by treating cells with HADA (hydroxyl coumarin-carbonyl amino-D-alanine), or with HALA (hydroxyl coumarin-carbonyl amino-L-alanine) as a negative control, essentially as described by Kuru et al. (29). A stock solution was added to the final 1-ml subculture to bring the culture to 0.5 mM in HADA or HALA and to 1% in dimethyl sulfoxide. The cells were harvested by centrifugation (1 min, 2,000 rpm), 0.9 ml of supernatant was removed, and the cells were resuspended in the remaining medium. To remove the excess HADA, the resulting suspension was applied to a microBio-Spin chromatography column packed with 0.1 g of Bio-Gel P-6GD (Bio-Rad Laboratories, Canada, Ltd., Mississauga, ON, Canada) in bacterial growth medium. The column was centrifuged at 2,000 rpm until no more cells were eluted.

Bright field, differential interference contrast (DIC), and fluorescence micrographs were obtained as described previously (28) with an Imaging RetigaEX or a Hamamatsu ORCA-R2 (C10600-10B) charge-coupled-device camera mounted on an Axiovert 200M inverted fluorescence microscope (Carl Zeiss Microimaging Inc.) equipped with a Zeiss Plan Neofluor 100×, numerical aperture 1.3, oil objective. To determine cell length distributions, ImageJ software was used to measure the lengths of 50 randomly selected, rod-shaped, nondividing cells (i.e., cells without invaginations) from each of two bright-field images (magnification, ×100; 100 cells in total). The contrast of all bright-field images was enhanced by increasing pixel saturation by 0.4%.

**SDS-PAGE and Western blotting.** SDS-PAGE (30) was performed with gels containing 12% (wt/vol) polyacrylamide and 1% (wt/vol) bisacrylamide (for detection of protein ProX) or 10% (wt/vol) polyacryl-

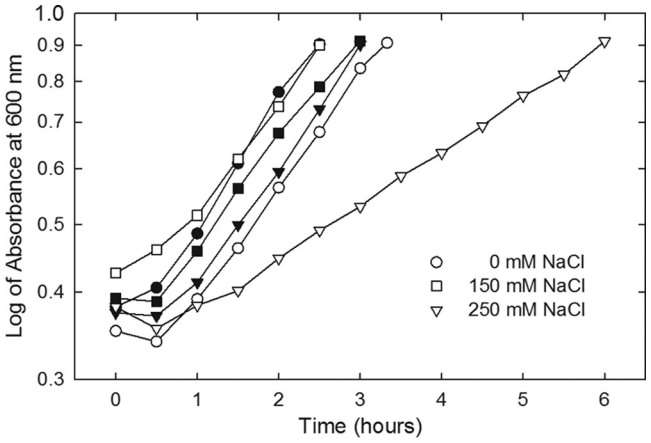


**FIG 1** Impact of mutation *proQ220*::Tn*5* on bacterial growth. *E. coli* strains WG170 (*proP*219 *proU*$^+$; closed symbols) and WG1074 (WG170 *proQ220*::Tn*5*; open symbols) were cultured in MOPS medium supplemented with no NaCl, 150 mM NaCl, or 250 mM NaCl. Bacterial growth was monitored by determining the optical density at 600 nm via a Bausch and Laumb Spectronic 88 spectrometer.

amide and 0.9% (wt/vol) bis-acrylamide (for detection of proteins ProQ and Prc). Tricine-SDS-PAGE (31) was performed with a separating gel containing 15.5% (wt/vol) polyacrylamide and 1% (wt/vol) bis-acrylamide (for detection of protein Lpp). Gels were stained with Gel-Code Blue (Pierce, Rockford, IL) according to the manufacturer's instructions. Western blotting was performed to detect ProX, ProQ, Prc, or Lpp, as described previously (32, 33). Western blots were visualized with enhanced chemiluminescence reagents (GE Healthcare, Baie d'Urfe, QC, Canada) according to the manufacturer's instructions.

## RESULTS

**High-salinity slows growth and elicits morphological defects in bacteria with *proQ* mutations.** The initial aim of this study was to further characterize the impacts of *proQ* lesions on the osmoregulatory systems of *E. coli*. It immediately became apparent that, in contrast to their *proQ*$^+$ parent, *proQ220*::Tn*5* bacteria grew very slowly at high salinity (Fig. 1, inverted closed versus inverted open triangles; doubling times of 1.9 h and 3.9 h, respectively). Strain WG1119 (Δ*proQ856*::*FRT*) also grew much more slowly at high salinity than its *proQ*$^+$ parent (data not shown). DIC microscopy revealed that bacteria with the *proQ* deletion were elongated after growth at low or high salinity (Fig. 2A). Long cells, swollen cells, enlarged spherical cells, and debris suggestive of cell lysis were evident in micrographs of the high-salinity cultures (Fig. 2, compare panels G and D). Highly refractive, eccentric internal structures were evident within many of the spherical cells (see Fig. S1E in the supplemental material). The spherical cells were viable, as indicated by BacLight staining, although they tended to lyse (data not shown).

**Lesions in *proQ* impair *prc* expression.** The *prc* locus follows *proQ* on the *E. coli* chromosome; the two are separated by only 20 bp, and a putative *prc* promoter is located within *proQ* (Fig. 3). Insertion *proQ220*::Tn*5* is upstream from the putative *prc* promoter, and deletion Δ*proQ856*::*FRT* removes it (Fig. 3). Bacteria with *prc* defects fail to grow at 42°C on solid ½L medium (NaCl-free, half-strength LB), and they form elongated cells when cultured at 42°C in liquid ½L medium (10). We had earlier concluded that the *proQ* transport phenotype did not result from effects of *proQ* mutations on *prc* expression, because those *prc* phenotypes were not shared by *proQ* mutant bacteria (9). This question was reconsidered in view of the observations reported above.

Unlike their *prc*$^+$ *proQ*$^+$ counterparts, bacteria with the mutation Δ*prc3*::*kan proQ220*::Tn*5* or Δ*proQ856*::*FRT* lacked the Prc protein (Fig. 4A). (Note that the band immediately below the Prc band, shared in all samples, represents a protein that is not related to Prc [M. Ehrmann, personal communication].) ProQ was absent from the *proQ* mutant bacteria, and the ProQ level increased with growth medium salinity, as expected (8). In addition, deletion of *prc* lowered the level of ProQ in bacteria cultivated at low or high salinity (Fig. 4B). Thus, *proQ* mutant bacteria are ProQ$^-$ Prc$^-$, and *prc* mutant bacteria are ProQ$^+$ Prc$^-$.

**Morphological phenotypes associated with Prc and ProQ deficiencies.** Further imaging and complementation analyses associated different morphological phenotypes with ProQ and Prc deficiencies. Fluorescence microscopy of bacteria with mutations in *prc* or *proQ* cultivated at high salinity (250 mM NaCl) revealed spherical cells bounded by FM4-64-stained membranes. Eccentric, DAPI-stained nucleoids within these cells were also surrounded by FM4-64-stained membranes (Fig. 5). Many of the spherical cells were much larger than the rod-shaped cells characteristic of wild-type *E. coli* (Fig. 5, compare with the images of *proQ*$^+$ *prc*$^+$ bacteria in the top right panel of Fig. 6A; bars designate 2.5 μm in both cases).

To identify the inner and outer membranes evident within the spherical cells, GFP variants targeted to the cytoplasm and periplasm were expressed in *proQ*$^+$ and *proQ* mutant bacteria. Periplasmic targeting via the twin-arginine translocase pathway was achieved by adding a 39-amino-acid TorA signal sequence as a tag to the N terminus of GFPmut2 (23). As expected, the untagged and tagged variants of GFPmut2 appeared in the cytoplasm and periplasm of wild-type, rod-shaped cells, respectively (data not shown). The untagged GFPmut2 variant colocalized with the DAPI-stained nucleoids of the spherical cells (Fig. 5, top panel), whereas the tagged variant appeared in the crescent-shaped region between the FM4-64-stained membranes (Fig. 5, bottom panel). Thus, the *proQ* morphological phenotype included increased cell size, loss of the characteristic rod shape, expansion of the periplasm, and cell lysis.

Complementation analysis to differentiate the *proQ* and *prc* mutant phenotypes was based on strain WG1119, in which Δ*proQ856*::*FRT* eliminates expression of both *proQ* and *prc*, and strain WG703 (*proQ*$^+$ Δ*prc3*::*kan*), which expresses *proQ* but not *prc* (Fig. 4). Complementation with a plasmid carrying *prc* (pCK3) restored Prc expression to both Δ*prc* and Δ*proQ* bacteria (Fig. 7D). In contrast, complementation with a plasmid carrying *proQ* (pDC77) restored *proQ* expression to Δ*proQ* bacteria (Fig. 7E), but it did not complement the Prc deficiency arising from effects of the chromosomal *proQ* mutation on *prc* (Fig. 7D). The levels of ProQ and Prc in bacteria harboring plasmids pDC77 and pCK3 were comparable to those in parent strain RM2 (*proQ*$^+$ *prc*$^+$) after cultivation in the same high-salinity medium (Fig. 7D and E).

Growth at high salinity caused bacteria lacking only *prc* (Δ*prc3*::*kan*) to form spherical cells (Fig. 2H and 5; see also Fig. S1F in the supplemental material) but not elongated rod-shaped cells (Fig. 2B). Plasmid-based expression of *prc* during

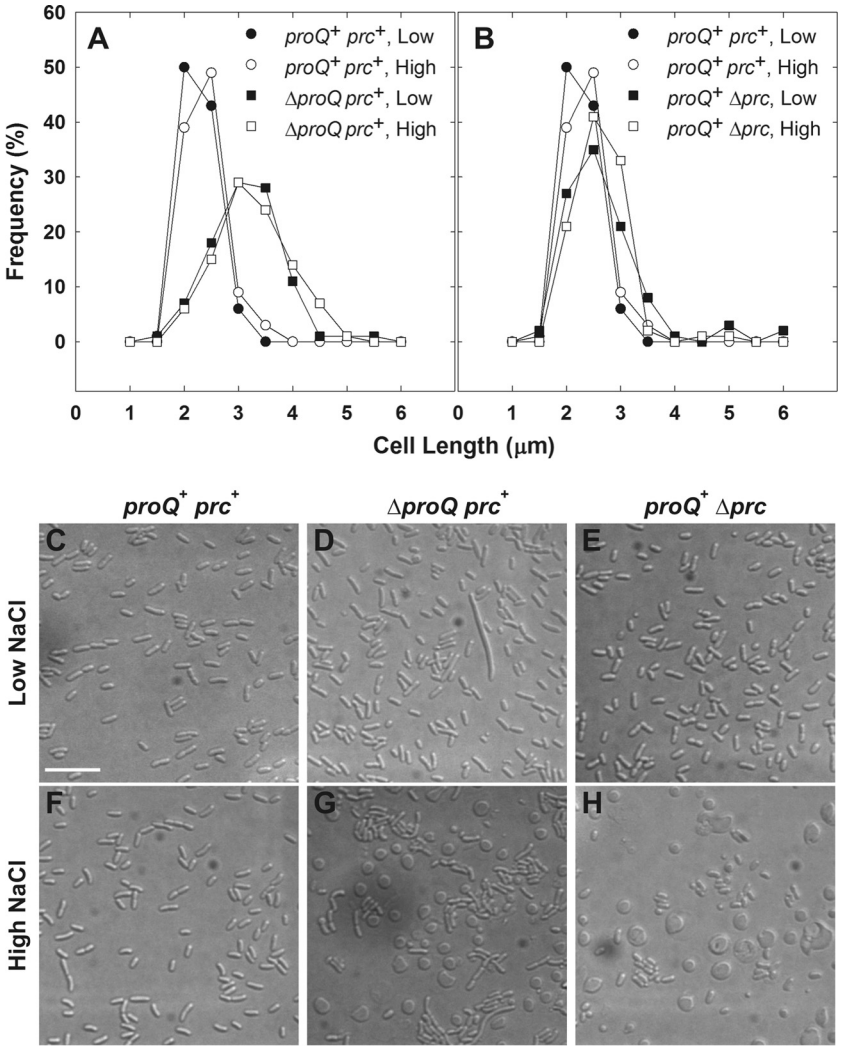


**FIG 2** Impacts of *proQ* and *prc* lesions on bacterial morphology. Bacteria were cultivated in MOPS medium to late exponential phase as described for transport assays (25) and visualized by DIC microscopy (see Materials and Methods). (A and B) Media were unsupplemented (0.25 mol $kg^{-1}$; closed symbols) or supplemented with 250 mM NaCl (0.75 mol $kg^{-1}$; open symbols). Length distributions are shown for 100 rod-shaped cells of strains RM2 (circles; *proQ*$^+$ *prc*$^+$) and WG1119 (squares; RM2 Δ*proQ856*::*FRT*) (A) and RM2 (circles) and WG703 (squares; RM2 Δ*prc3*::*kan*) (B). Subsequent experiments revealed that Δ*proQ856*::*FRT* renders the bacteria ProQ and Prc deficient (see Fig. 4). For strain WG1119, 3% of measured cells in cultures at low osmolality and 4% of measured cells in cultures at high osmolality were greater than 6 μm in length. No measured cells in cultures of strain RM2 or WG703 at low or high osmolality were greater than 6 μm in length. (C to H) Representative DIC micrographs are shown for strains RM2 (C and F), WG1119 (D and G), and WG703 (E and H) cultivated in unsupplemented medium (low NaCl; C, D, and E) or NaCl-supplemented medium (high NaCl; F, G, and H). Spherical cells with highly refractive, crescent-shaped internal structures are evident in panels G and H. (In Fig. S1 in the supplemental material, the internal structures are more evident in the corresponding panels [E and F].) Bars, 10 μm.

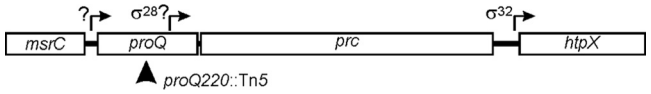


**FIG 3** Organization of *proQ*, *prc*, and flanking loci The *prc* locus follows *proQ* on the *E. coli* chromosome. A putative $\sigma^{28}$ promoter for *prc*, with a predicted transcription start site at nucleotide (nt) 1,913,051, falls within the *proQ* open reading frame (nt 1,912,860 to 1,913,558) (10, 60). Insertion *proQ220*::Tn*5* is upstream from the putative *prc* promoter (9), whereas deletion Δ*proQ856*::*FRT* removes it (the start codon and the final six codons are retained [16]). A *proQ-prc* transcript may initiate upstream of *proQ* (61). No promoter or transcription start site has been identified for upstream locus *msrC* (also known as *yebR*), which encodes a methionine-(*R*)-sulfoxide reductase (75). Independent transcription of the downstream *htpX* locus is mediated by $\sigma^{32}$ (76).

growth of *E. coli* WG1119 at high salinity eliminated spherical cells and restored a more normal growth rate (a doubling time of 2.6 h) but not a normal cell length distribution (Fig. 7A). Thus, the formation of spherical cells was due to Prc deficiency, whereas cell elongation was associated with ProQ deficiency.

Plasmid-based expression of *proQ* restored a more normal cell length distribution (Fig. 7B) and growth rate to Δ*proQ856*::*FRT* bacteria grown at high salinity (the doubling times for strains WG1119 and WG1119 pDC77 were 3.3 h and 2.8 h, respectively), but it did not eliminate spherical cells (Fig. 7B). This was expected, since the bacteria remained Prc deficient (Fig. 7D). With both plasmids, cell morphology became normal (Fig. 7C) but culture growth was still impaired (doubling time, 3.6 h). These results

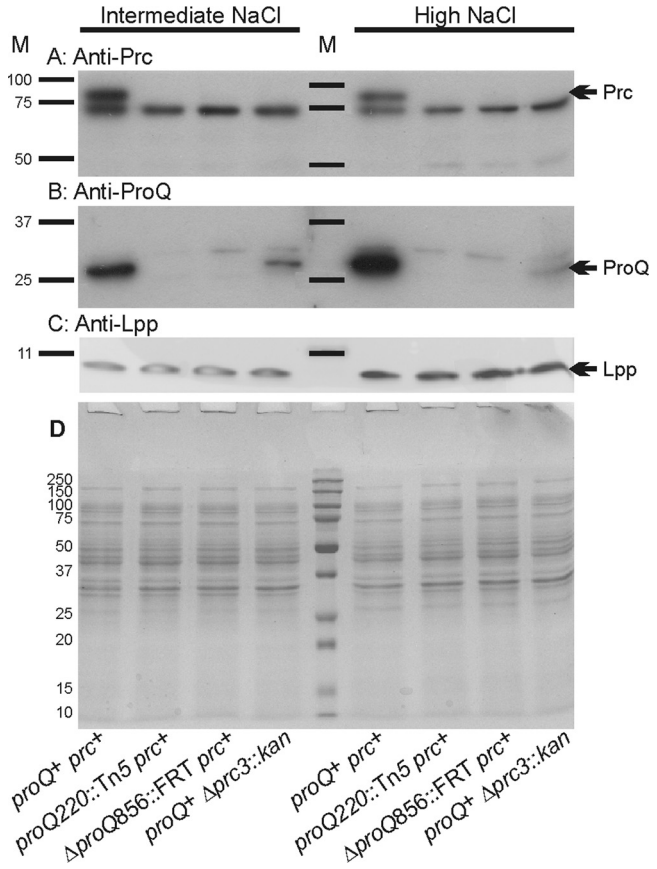


**FIG 4** Impacts of *proQ* and *prc* lesions on Prc, ProQ, and Lpp protein levels. *E. coli* strains RM2 (*proQ*$^+$ *prc*$^+$), WG174 (RM2 *proQ220*::Tn*5* [phenotypically ProQ$^-$ Prc$^-$]), WG1119 (RM2 Δ*proQ856*::*FRT* [phenotypically ProQ$^-$ Prc$^-$]), and WG703 (RM2 Δ*prc3*::*kan* [phenotypically ProQ$^+$ Prc$^-$]) were grown in MOPS medium supplemented with 120 mM NaCl (intermediate NaCl) or 250 mM NaCl (high NaCl). Aliquots of cell extracts containing 15 μg of protein were analyzed by Western blotting to detect Prc (A) or ProQ (B), and aliquots containing 1.5 μg of cell protein were analyzed to detect Lpp (C). In panel A, the band immediately below Prc, shared in all samples, represents a protein that is not related to Prc (M. Ehrmann, personal communication). Panel D shows a corresponding GelCode Blue-stained SDS-PAGE gel. M, molecular weight markers; arrows, locations of Prc, ProQ, and Lpp.

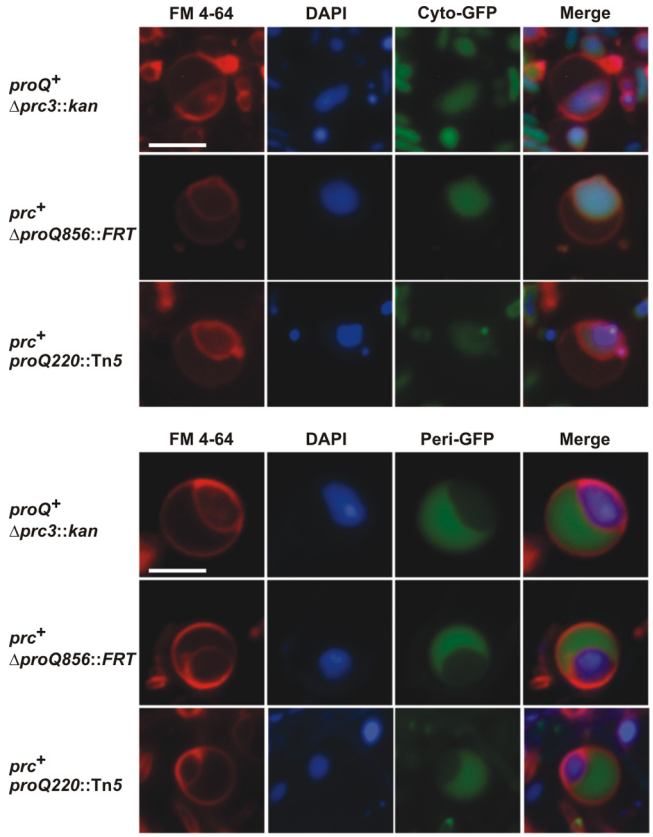


**FIG 5** Bacteria with mutations in *proQ* or *prc* form spherical cells at high salinity. Derivatives of *E. coli* strains WG703 (Δ*prc3*::*kan*), WG1119 (Δ*proQ856*::*FRT*), and WG174 (*proQ220*::Tn*5*) containing plasmid pMGS053 (carrying the gene for cytoplasmic green fluorescent protein [Cyto-GFP]) or plasmid pJW1 (carrying the gene for periplasmic GFP [Peri-GFP]) were cultivated in MOPS medium supplemented with 250 mM NaCl as described in the legend for Fig. 2. Cells from late-exponential-phase cultures were stained with DAPI (the nucleoid; blue fluorescence) and FM4-64 (the membranes; red fluorescence). Micrographs of representative spherical cells are shown. Bar, 2.5 μm.

confirmed that cell elongation results from consequences of *proQ* defects other than Prc deficiency.

**Origins of spherical cell formation by *prc* mutant bacteria.** HADA is a fluorescent analogue that is incorporated into peptidoglycan in place of D-alanine (29). To locate the murein layer in Prc-deficient cells, strains WG1119 (Δ*proQ856*::*FRT prc*$^+$) and WG703 (*proQ*$^+$ Δ*prc3*::*kan*) were labeled with HADA during growth in high-salinity medium. Blue HADA fluorescence corresponded with the inner ring of red FM4-64 fluorescence in cells from both cultures (Fig. 6B). Treatment of the bacteria with the L-stereoisomer HALA (29) yielded weak, background fluorescence under these conditions. These results suggest that the murein layer in these bacteria surrounds their inner, cytoplasmic compartment, and the space between the outer membrane and murein layer is enlarged.

Detachment of the outer membrane from the murein layer could in principle result from absence or degradation of the murein lipoprotein (Lpp). Estimated to be the most abundant *E. coli* protein, Lpp exists in two forms. The transmembrane form is embedded in the outer membrane, whereas the lipid moiety of the periplasmic form is embedded in the inner leaflet of the outer membrane, and its C terminus is cross-linked to the murein layer (34). We reasoned that the *proQ* morphological phenotype might result from Lpp deficiency, which is known to cause spheroid cell formation (35) and outer membrane blebbing (36). Similar levels of Lpp were detected by Western blotting of cell extracts from wild-type bacteria and from those with *proQ* and/or *prc* mutations (Fig. 4C). No degradation of this protein was evident. Thus, the *proQ* morphological phenotype did not result from an absence of Lpp.

MreB is required for maintenance of the rod shape of *E. coli* cells (reviewed in references 37 and 38). We reasoned that *proQ* mutations may affect cell morphology by affecting MreB, which can be specifically inhibited by A-22 (39, 40). A-22-treated, ProQ$^+$ Prc$^+$ cells were spherical, with concentric membrane layers (Fig. 6A). They were much smaller and more symmetrical than those resulting from *proQ* defects (Fig. 5). Thus, the morphological phenotypes associated *proQ* mutations were distinct from those elicited by A-22.

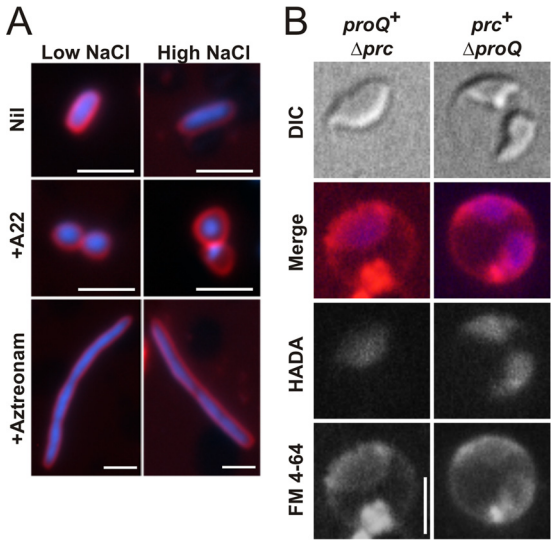


**FIG 6** Determinants of bacterial morphology. (A) Impacts of A-22 and aztreonam on the morphology of *E. coli*. Strain RM2 (*proQ*$^+$ *prc*$^+$) was cultivated in MOPS medium without or with 250 mM NaCl (low NaCl or high NaCl) and without or with A-22 (5 μg/ml) or aztreonam (1 μg/ml) as described in Materials and Methods. Cells were stained with DAPI (the nucleoid; blue fluorescence) and FM4-64 (the membranes; red fluorescence), and images were obtained as described in Materials and Methods. Bars, 2.5 μm. (B) Location of the peptidoglycan layer. Bacteria were cultivated in MOPS medium with 250 mM NaCl (high NaCl) in the presence HADA (peptidoglycan; blue fluorescence) and stained with FM4-64 (membranes; red fluorescence) as described in Materials and Methods. Bars, 2.5 μm.

PBP3 (also known as FtsI) is required for septation of *E. coli* cells (reviewed in references 37 and 38). Prc cleaves the periplasmic C termini of PBP3 (10) and lipoprotein NlpI (63). Aztreonam specifically inhibits the transpeptidase activity of PBP3, disrupting septal murein synthesis and elongating cells (41, 42, 64). Cleavage of PBP3 by Prc is not essential for bacterial growth and morphogenesis at low salinity (Fig. 2E). To determine whether cleavage by Prc is important for PBP3 activity during bacterial growth at high salinity, bacteria lacking Prc but not ProQ (Fig. 2H and 5) were compared with ProQ$^+$ Prc$^+$ bacteria in which aztreonam inhibited PBP3 during growth at high salinity (Fig. 6A). These cells were very different (spheres versus filaments), so we concluded that the phenotype of Prc-deficient bacteria cultivated at high salinity does not arise because cleavage of PBP3 by Prc is required for PBP3 activity at high salinity.

Spr is a murein D,D-endopeptidase, one of three murein hydrolases that are redundantly essential for cleavage of peptidoglycan cross-links, allowing insertion of new material and enlargement of the murein sacculus of *E. coli* (43). Mutations in *spr* restore the growth of *prc* mutant bacteria at high temperature and low osmolality (43, 44). Deletion of *spr* also restored a more normal growth rate and suppressed spherical cell formation by Δ*prc3*::*kan* bacteria at high salinity (Fig. 8B and H). Thus, the spherical cell phenotype of Prc-deficient bacteria may result at least in part from uncontrolled Spr activity.

**ProQ and Prc deficiencies affect ProP differently but do not affect other osmoregulatory systems.** The *proQ* locus was originally identified via effects of *proQ* lesions on ProP activity (45, 46), so the effects of *proQ* lesions on transporter ProP are well characterized (8, 9, 47). The intial aim of this study was to define the effects of ProQ deficiency on other osmoregulatory functions. For *E. coli* K-12, cultivation in high-osmotic pressure medium activates trehalose accumulation mediated by trehalose-6-phosphate synthase (OtsA) and phosphatase (OtsB). The accumulation of other osmolytes can be mediated by transporters ProP, ProU, and BetT. ProU is an ABC transporter encoded by the *proU* operon and comprised of an ATP-binding cassette (ProV) and membrane-integral (ProW) and periplasmic (ProX) subunits. ProP and ProU transport proline, glycine betaine, and related compounds, whereas choline is the primary BetT substrate (48).

The impacts of a *proQ* defect on transporter ProU were assessed, because independent work had revealed suppression of the *proQ* transport phenotype by deletions within the *proU* operon (49). Insertion *proQ220*::Tn*5* did not affect either glycine betaine uptake via ProU (Fig. 9A) or the level of the ProX protein (Fig. 9B), despite dramatically attenuating bacterial growth (Fig. 1). This was consistent with a previous report based on qualitative data (46).

*E. coli* was cultivated at high salinity without organic osmoprotectants to induce *proU* expression for measurements of ProU activity (Fig. 9A). Under these conditions, *E. coli* can also osmoregulate by accumulating $K^+$-glutamate and then replacing that salt with trehalose (50, 51). A compound with the $R_f$ of trehalose was detected upon chromatographic analysis of cell extracts prepared from both *proQ*$^+$ and *proQ* mutant bacteria after cultivation at high salinity (Fig. 9C). As expected, that material was not detected in extracts from bacteria cultivated at low salinity (Fig. 9C). Thus, the slow growth (Fig. 1) and morphological phenotypes (Fig. 2 and 5) of *proQ* mutant strain bacteria did not result from failure to accumulate trehalose.

The impacts of ProQ and Prc deficiencies on ProP activity were also reevaluated. In previous work, radial streak tests revealed no impact of Δ*prc3*::*kan* on ProP activity (9). Transport assays confirmed that ProP activity was not eliminated by the *prc* mutation, but ProP activity was lowered and its dependence on assay medium osmolality was altered (Fig. 10A). The bacteria used for these assays were cultured at an intermediate salinity that is optimal for ProP expression and function (MOPS medium with 0.12 M NaCl) but does not elicit spherical cell formation. Complementation with plasmid-harbored Prc fully restored Prc expression (Fig. 7D) and ProP activity (Fig. 10B). Lesions within *proQ*, which block expression of *proQ* and *prc*, impaired ProP activity more severely than did *prc* defects (Fig. 10A) (9). Complementation with plasmid-encoded ProQ restored expression of ProQ (Fig. 7E) but not Prc (Fig. 7D), and it restored ProP activity only to levels characteristic of *prc* mutant bacteria (Fig. 10C). Thus, both ProQ and Prc are required for full ProP activity under conditions that do not elicit spherical cell formation. ProQ and Prc are not required by other osmoregulatory systems (trehalose synthesis or glycine betaine transport via ProU [Fig. 9]).

**Glycine betaine accumulation suppresses phenotypes associated with ProQ but not Prc deficiency.** The data discussed above show that both ProQ and Prc are required for normal cell growth at high salinity. To further explore the relationship between the *proQ* transport and morphological phenotypes, we determined the impact of ProP-mediated glycine betaine accumulation on the morphological phenotypes. Cell length returned to the normal range (see Fig. S2 in the supplemental material), and the incidence of spherical cells was dramatically reduced when bacteria lacking ProQ and Prc were cultivated in glycine betaine-sup-

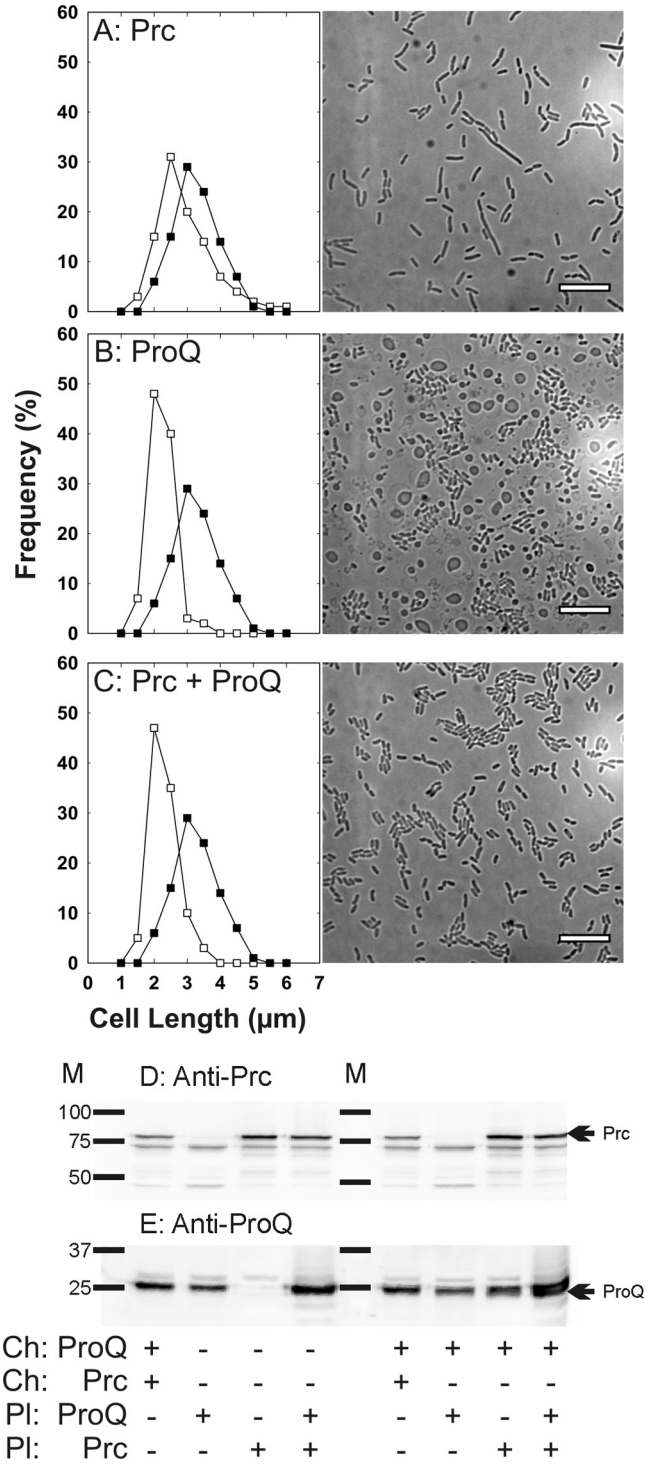


**FIG 7** Complementation of Prc- and ProQ-deficient *E. coli* strains with plasmids carrying genes for Prc and ProQ. Bacteria were cultivated in MOPS medium supplemented with 250 mM NaCl (0.75 mol $kg^{-1}$) to late exponential phase as described for transport assays (25) (A to C) The bacteria were visualized by light microscopy (see Materials and Methods). Cell length distributions and representative light micrographs are shown for WG1119 pCK3 (restoring Prc but not ProQ; open squares) A), WG1119 pDC77 (restoring ProQ but not Prc; open squares) (B), and WG1119 pDC77 pCK3 (restoring ProQ and Prc; open squares) (C) in comparison with WG1119 (lacking ProQ and Prc; closed squares) for all cases. Bars, 10 μm. (D and E) An aliquot of the cell extract from each culture (15 μg of protein) was analyzed by Western blotting to detect Prc (D) or ProQ (E). Strain RM2 (*proQ*$^+$ *prc*$^+$) was included to illustrate the levels of ProQ and Prc attained when each is encoded by its chromosomal gene. To test the levels of expression of these proteins from the plasmid-borne genes, plasmids pCK3 (for Prc) or pDC77 (for ProQ) or both were introduced to strain WG1119 (which otherwise lacks both proteins) (left lanes), or the same plasmids were introduced to strain WG703 (which otherwise lacks Prc but not ProQ) (right lanes). M, molecular weight markers; arrows, locations of ProQ and Prc.

plemented, high-salinity medium (see Fig. S1 in the supplemental material; compare panels H and E). Notably, the accumulation of $K^+$-glutamate and trehalose did not have this effect (Fig. 2A and G). In contrast, glycine betaine did not suppress spherical cell formation by bacteria lacking only Prc (see Fig. S1, compare panels F and I). Glycine betaine is much more effective than trehalose in restoring the hydration of *E. coli* cells under osmotic stress (2, 52–54). These data suggest that cellular dehydration and Prc deficiency have distinct effects on bacterial morphology.

## DISCUSSION

ProQ is a soluble, cytoplasmic protein with a trypsin-sensitive linker that connects trypsin-resistant N- and C-terminal domains (residues 1 to 131 and 170 to 232, respectively) (47). These domains are structural homologues of RNA-binding translational regulators FinO (47) and Hfq (8), respectively. FinO regulates F-pilus biogenesis by binding small RNA (sRNA) FinP (55–57), while Hfq is a pleiotrophic regulator with multiple sRNA partners (58). No physiological RNA targets of ProQ have been found (49), but ProQ exerts RNA chaperone activities on FinO substrates. The FinO-like ProQ domain binds RNA with high affinity, and the Hfq-like ProQ domain facilitates RNA strand exchange and duplexing (8).

Prc is an ATP-dependent periplasmic protease with an N-terminal domain of unknown function, a central PDZ domain, and a C-terminal serine protease domain (682 residues in total) (59). Prc was designated a tail-specific protease (Tsp) because it cleaves protein C termini in a sequence-dependent manner (11, 59). Only 20 nucleotides separate *prc* from *proQ* (Fig. 3). A putative *prc* promoter was identified within *proQ* (10, 60), but Prc was not detected in bacteria with a Tn*5* insertion in *proQ*, 122 bp upstream from the putative *prc* transcription start site (allele *proQ220*::Tn*5*) (Fig. 4A). A *proQ-prc* transcript was identified (61), mutations in *proQ* eliminated Prc (Fig. 4A), and replacement of *prc* lowered ProQ levels (allele Δ*prc3*::*kan*) (Fig. 4B). These data suggest that *proQ* and *prc* are cotranscribed (Fig. 3), and the reciprocal effects of *proQ* and *prc* mutations (Fig. 4) result from alteration of a *proQ-prc* transcript. ProQ may act as an RNA chaperone to regulate translation of a *proQ-prc* mRNA.

This study linked ProQ deficiency with cell elongation (Fig. 2 and 7). That elongation was reversed by the osmoprotectant glycine betaine (see Fig. S2 in the supplemental material) but not by accumulation of trehalose (Fig. 2A and 9). Glycine betaine is more effective than trehalose at restoring the hydration of bacteria cultivated at high salinity (53). Diverse perturbations cause cells to elongate. They include the SOS response, a variety of cell division defects, and the inhibition of cell division proteins (e.g., aztreonam inhibition of PBP3 [Fig. 6A]). The mechanism by which ProQ deficiency causes cell to elongate is not currently known.

No morphological phenotype is evident for bacteria lacking Prc but not ProQ during growth in standard media with optimal

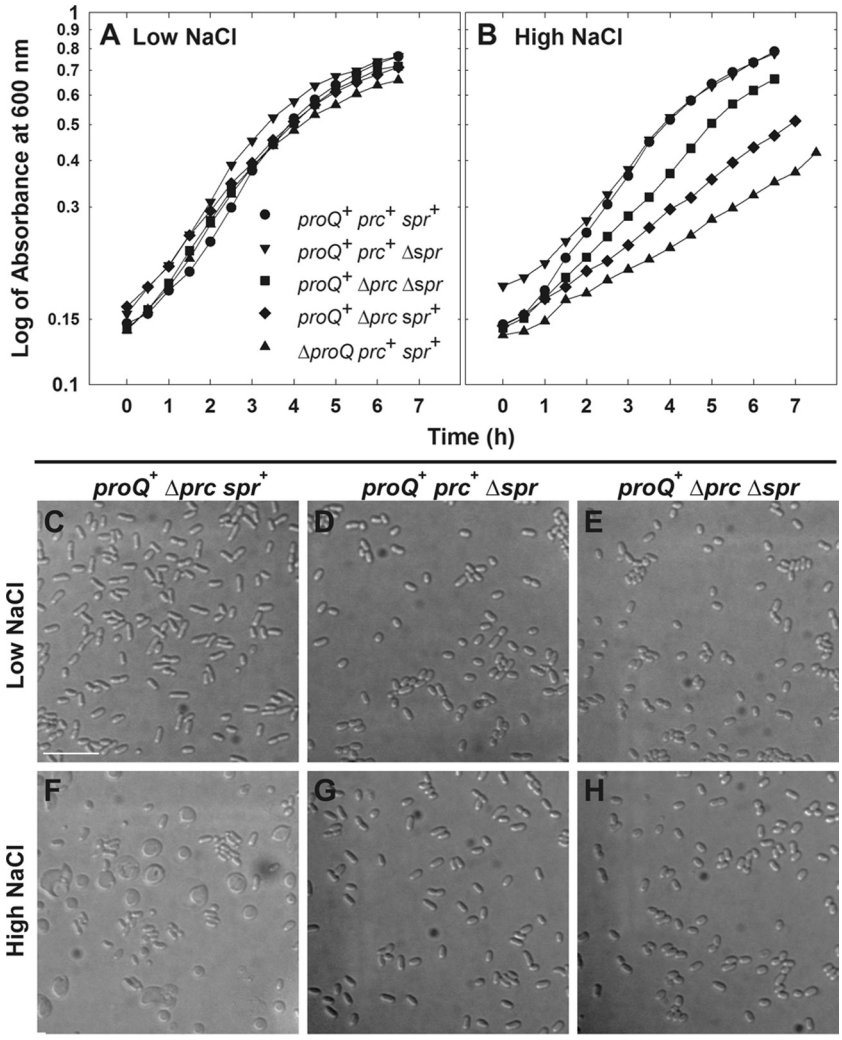


**FIG 8** Deletion of *spr* suppresses the *prc* morphological phenotype. Bacteria were cultivated in MOPS medium to late exponential phase as described for transport assays (25) and visualized by DIC microscopy (see Materials and Methods). Media were unsupplemented (0.25 mol $kg^{-1}$, low NaCl) (A) or supplemented with 250 mM NaCl (0.75 mol $kg^{-1}$; high NaCl) (B). Culture optical densities (at 600 nm) were measured with a Pharmacia Novaspec II spectrometer. Representative DIC micrographs are shown for strains WG703 (*proQ*$^+$ Δ*prc3*::kan *spr*$^+$ [C and F]), WG1457 (*proQ*$^+$ *prc*$^+$ Δ*spr832*::*FRT* [D and G]), and WG1458 (*proQ*$^+$ Δ*prc3*::*kan* Δ*spr832*::*FRT* [E and H]). Bars, 10 μm.

salinities (Fig. 2B and E). However, *prc* mutant bacteria grow slowly and form filaments during cultivation in rich media at very low salinity and high temperature (10, 62), and they form spherical cells with an enlarged periplasm and eccentric cytoplasm upon cultivation at the optimal temperature (37°C) and high salinity (Fig. 2H and 5). The spherical cells form despite the accumulation of trehalose (Fig. 9) or the provision of glycine betaine (see Fig. S1I in the supplemental material).

Previous observations have linked Prc to cell division and periplasmic protein quality control. The morphological consequences of Prc deficiency for bacteria cultivated at high salinity reported here (Fig. 2 and 5; see also Fig. S1 in the supplemental material) did not correlate with morphological changes resulting from A-22 inhibition of MreB or aztreonam inhibition of PBP3 (Fig. 6A). However, an *spr* deletion suppressed the growth and morphological phenotypes associated with cultivation of Prc-deficient bacteria at low (44) or high (Fig. 8) salinity. Spr is predicted to associate with the outer membrane of *E. coli* via an N-terminal signal peptidase recognition sequence, culminating in a membrane-anchoring cysteine. The structure of the C-terminal domain of Spr confirms its membership in the NlpC/P60 protein domain family of peptidases (65), and the murein D,D-endopeptidase activity of that periplasmic domain contributes to enlargement of the murein sacculus (43). Our observations suggest that a Prc deficiency promotes uncontrolled Spr activity, cell rounding, loss of murein layer integrity, and ultimately cell lysis when bacteria are cultivated at high salinity. This hypothesis is consistent with a variety of observations linking the PDZ and serine protease domains of Prc to protein quality control (10–14, 33, 66). A *tsp* (*prc*) mutation produced synthetic phenotypes with *degP*, *ppiD*, *surA*, *fkpA*, and *ydgD*, each with a known or putative role in protein quality control. In addition, bacteria with defects at *surA*, *dsbA*, and various combinations of quality control or protease loci grew poorly at high salinity (33).

Like the osmotic stress-dependent morphological phenotypes, the distinct effects of ProQ and Prc deficiencies on the activity of

A

| Strain | Relevant Genotype | Glycine Betaine Uptake Rate | |
|---|---|---|---|
| | | Bacteria Grown with NaCl at: | |
| | | 150 mM | 250 mm |
| WG170 | *proQ*$^+$ | 12 ± 0.5 | 22 ± 0.1 |
| WG1074 | *proQ220*::Tn*5* | 11 ± 0.1 | 26 ± 0.3 |

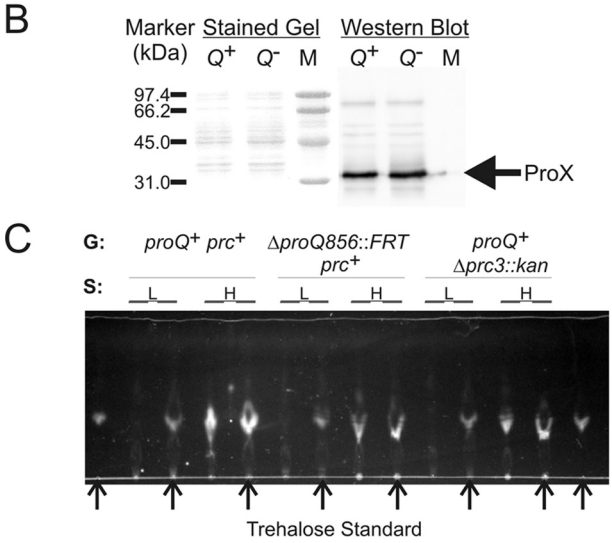


**FIG 9** Impacts of mutations *proQ220*::Tn*5* and Δ*prc3*::*kan* on ProU activity, ProX levels, and trehalose accumulation. (A and B) *E. coli* strains WG170 (*proP*219 *proU*$^+$) and WG1074 (WG170 *proQ220*::Tn*5* [phenotypically ProQ$^-$ Prc$^-$]) were cultured in MOPS medium supplemented with no NaCl, 150 mM NaCl, or 250 mM NaCl. These strains were used because they lack ProP, which also transports glycine betaine. Glycine betaine uptake activity was measured (A), and the ProX levels in bacteria cultivated in MOPS medium with 250 mM NaCl were determined by Western blotting (B). Each procedure was performed as described in Materials and Methods. No glycine betaine uptake by either strain could be detected after cultivation in MOPS medium without supplementary NaCl. Q$^+$ and Q$^-$ designate cell extracts from *proQ*$^+$ and *proQ* mutant strain bacteria, respectively. M designates markers with the indicated molecular weights, and the arrow designates the electrophoretic mobility of the ProX protein. (C) *E. coli* strains RM2 (*proQ*$^+$ *prc*$^+$), WG1119 (Δ*proQ856*::*FRT* [phenotypically ProQ$^-$ Prc$^-$]), and WG703 (*proQ*$^+$ Δ*prc3*::*kan* [phenotypically ProQ$^+$ Prc$^-$]) were grown in MOPS medium without (L) or with (H) 250 mM NaCl, metabolites were extracted, and the extracts were analyzed by TLC as described in Materials and Methods. G, genotype. Arrows denote samples to which trehalose (5 nmol) was added as a standard.

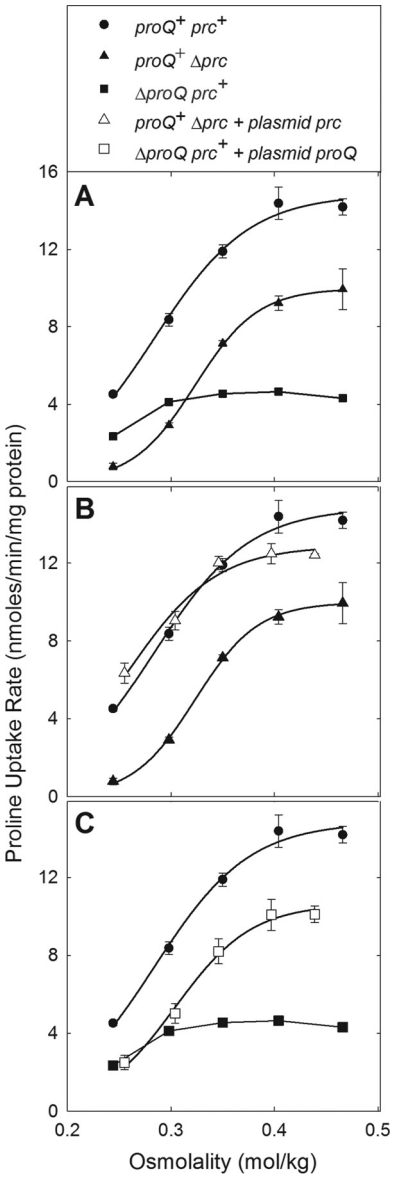


**FIG 10** ProQ and Prc deficiencies alter ProP activity differently. *E. coli* strains RM2 (*proQ*$^+$ *prc*$^+$), WG1072 (RM2 Δ*proQ756*::*kan* [phenotypically ProQ$^-$ Prc$^-$]), WG1414 (WG1072 pDC77 [phenotypically ProQ$^+$ Prc$^-$]), WG703 (RM2 Δ*prc3*::*kan* [phenotypically ProQ$^+$ Prc$^-$]), and WG1371 (WG703 pCK3 [phenotypically ProQ$^+$ Prc$^+$]) were cultivated in MOPS medium, and proline uptake rates were measured as a function of the assay medium osmolality, as described in Materials and Methods. Plasmid pDC77 encodes ProQ and pCK3 encodes Prc. For strains RM2 and WG703, nonlinear regression (performed with SigmaPlot) was used to fit the initial rate of proline uptake ($a_0$) at the corresponding assay medium osmolality ($\Pi$/RT) to the following equation: $a_0 = A_{max}/[1 + e^{-(\Pi-\Pi_{1/2})/RTB}]$, where $a_0$ is the initial rate of substrate (radiolabeled proline) uptake, $A_{max}$ is the rate that would be attained at infinite osmolality, B is a constant, $\Pi_{1/2}$/RT is the value of $\Pi$/RT at which $a_0 = \frac{1}{2}A_{max}$, R is the gas constant (8.314 J · K$^{-1}$ · mol$^{-1}$), and *T* is the temperature (298°K). ProP activity was half-maximal at an osmolality of 284 ± 6 mmol/kg for RM2 and 323 ± 6 mmol/kg for WG703 (means ± standard errors).

the osmoregulatory transporter ProP link ProQ and Prc to the osmotic stress response. However ProQ and Prc are not general effectors of the osmoregulatory response, since their absence did not impair other osmoregulatory functions (osmoprotectant transport via ProU and trehalose synthesis mediated by OtsAB [Fig. 9]). ProP activity is a sigmoid function of the assay medium osmolality. The amplitude of the osmotic activation response reflects the expression level of ProP. The 3- to 4-fold decrease in amplitude of the osmotic activation response in ProQ-deficient bacteria (Fig. 10A) was consistent with the previously reported effect of ProQ deficiency on ProP levels (8, 9).

The following observations suggest that Prc deficiency may affect ProP function by altering cell structure. The osmolality at which ProP activity is half maximal ($\Pi_{1/2}$/RT [Fig. 10 legend]) is directly proportional to the anionic phospholipid content of the membrane in which ProP resides (67, 68). Prc deficiency lowers the amplitude of the osmotic activation response approximately 30% and raises the osmolality required to reach half maximal activity (Fig. 10A, legend). Cardiolipin concentrates at the poles of *E. coli* cells and ProP concentrates at the cell poles in a cardiolipin-

dependent manner, whereas the membrane-integral ProW component of the ProU system does not (28, 68, 69). The effects of Prc deficiency on ProP activity occur in bacteria cultivated at moderate salinities that do not elicit spherical cell formation. Thus, ProP may indicate subtle effects of Prc deficiency on cell wall and cytoplasmic membrane organization that occur under these moderate conditions.

## ACKNOWLEDGMENTS

We are grateful to Eric Brown (McMaster University) for Keio Collection isolates, to Michelle N. Smith-Frieday (University of Guelph) for creating *Escherichia coli* strains WG1072, WG1074, and WG1119, to France-Isabelle Auzanneau for advice on thin-layer chromatography, to Merna Villarejo (University of California, Davis), Michael Ehrmann (University of Duisburg-Essen, Germany), and Hajime Tokuda (University of Morioka, Japan) for anti-ProX, anti-Prc, and anti-Lpp antibodies, respectively, to James Weisshaar (University of Wisconsin—Madison) for plasmids pMGS053 and pJW1, to Cezar Khursigara for A-22, and to Erkin Kuru and Michael Van Nieuwenhze (Indiana University) for HADA and HALA.

We acknowledge the Natural Sciences and Engineering Research Council of Canada for a Discovery Grant awarded to J.M.W.

## REFERENCES

1. **Altendorf K, Booth IR, Gralla JD, Greie J-C, Rosenthal AZ, Wood JM.** 2009. Osmotic stress. EcoSal Plus http://dx.doi.org/10.1128./ecosalplus.5.4.5.
2. **Cayley DS, Guttman HJ, Record MT, Jr.** 2000. Biophysical characterization of changes in amounts and activity of *Escherichia coli* cell and compartment water and turgor pressure in response to osmotic stress. Biophys. J. **78:**1748–1764. http://www.ncbi.nlm.nih.gov/pmc/articles/PMC1300771/.
3. **Koch AL, Woeste S.** 1992. Elasticity of the sacculus of *Escherichia coli*. J. Bacteriol. **174:**4811–4819.
4. **Wood JM.** 2010. Osmotic stress, p 133–156. *In* Storz G, Hengge R (ed), Bacterial stress responses, 2nd ed. ASM Press, Washington, DC.
5. **Wood JM.** 2007. Bacterial osmosensing transporters. Methods Enzymol. **428:**77–107. http://dx.doi.org/10.1016/S0076-687(07)28005-X.
6. **MacMillan SV, Alexander DA, Culham DE, Kunte HJ, Marshall EV, Rochon D, Wood JM.** 1999. The ion coupling and organic substrate specificities of osmoregulatory transporter ProP in *Escherichia coli*. Biochim. Biophys. Acta **1420:**30–44.
7. **Culham DE, Lu A, Jishage M, Krogfelt KA, Ishihama A, Wood JM.** 2001. The osmotic stress response and virulence in pyelonephritis isolates of *Escherichia coli*: contributions of *rpoS*, *proP*, *proU* and other systems. Microbiology **147:**1657–1670. http://mic.sgmjournals.org/content/147/6/1657.long.
8. **Chaulk SG, Smith-Frieday MN, Arthur DC, Culham DEERA, Soo P, Frost LS, Keates RAB, Glover JN, Wood JM.** 2011. ProQ is an RNA chaperone that controls ProP levels in *Escherichia coli*. Biochemistry **50:**3095–3106. http://dx.doi.org/10.1021/bi101683a.
9. **Kunte HJ, Crane RA, Culham DE, Richmond D, Wood JM.** 1999. Protein ProQ influences osmotic activation of compatible solute transporter ProP in *Escherichia coli* K-12. J. Bacteriol. **181:**1537–1543.
10. **Hara H, Yamamoto Y, Higashitani A, Suzuki H, Nishimura Y.** 1991. Cloning, mapping, and characterization of the *Escherichia coli prc* gene, which is involved in C-terminal processing of penicillin-binding protein 3. J. Bacteriol. **173:**4799–4813.
11. **Silber KR, Keiler KC, Sauer RT.** 1992. Tsp: a tail-specific protease that selectively degrades proteins with nonpolar C termini. Proc. Natl. Acad. Sci. U. S. A. **89:**295–299.
12. **Seoane A, Sabbaj A, McMurry LM, Levy SB.** 1992. Multiple antibiotic susceptibility associated with inactivation of the *prc* gene. J. Bacteriol. **174:**7844–7847.
13. **Bass S, Gu Q, Christen A.** 1996. Multicopy suppressors of *prc* mutant *Escherichia coli* include two HtrA (DegP) protease homologs (HhoAB), DksA, and a truncated R1pA. J. Bacteriol. **178:**1154–1161.
14. **Beebe KD, Shin J, Peng J, Chaudhury C, Khera J, Pei D.** 2000. Substrate recognition through a PDZ domain in tail-specific protease. Biochemistry **39:**3149–3155. http://dx.doi.org/10.1021/bi992709s.
15. **Baba T, Ara T, Hasegawa M, Takai Y, Okumura Y, Baba M, Datsenko KA, Tomita M, Wanner BL, Mori H.** 2006. Construction of *Escherichia coli* K-12 in-frame, single-gene knockout mutants: the Keio collection. Mol. Syst. Biol. **2:**2006.0008. http://dx.doi.org/10.1038/msb4100050.
16. **Datsenko KA, Wanner BL.** 2000. One-step inactivation of chromosomal genes in *Escherichia coli* K-12 using PCR products. Proc. Natl. Acad. Sci. U. S. A. **97:**6640–6645. http://dx.doi.org/10.1073/pnas.120163297.
17. **Miller JH.** 1972. Experiments in molecular genetics. Cold Spring Harbor Laboratory, Cold Spring Harbor, NY.
18. **Hanahan D.** 1983. Studies on transformation of *Escherichia coli* with plasmids. J. Mol. Biol. **166:**557–569.
19. **Sambrook J, Russell DW.** 2001. Molecular cloning: a laboratory manual. Cold Spring Harbor Laboratory Press, Cold Spring Harbor, NY.
20. **Brown ED, Wood JM.** 1992. Redesigned purification yields a fully functional PutA protein dimer from *Escherichia coli*. J. Biol. Chem. **267:**13086–13092.
21. **Guzman L-M, Belin D, Carson MJ, Beckwith J.** 1995. Tight regulation, modulation, and high-level expression by vectors containing the arabinose $P_{BAD}$ promoter. J. Bacteriol. **177:**4121–4130.
22. **Elowitz MB, Surette MG, Wolf PE, Stock JB, Leibler S.** 1999. Protein mobility in the cytoplasm of *Escherichia coli*. J. Bacteriol. **181:**197–203.
23. **Sochacki KA, Shkel IA, Record MT, Weisshaar JC.** 2011. Protein diffusion in the periplasm of *E. coli* under osmotic stress. Biophys. J. **100:**22–31. http://dx.doi.org/10.1016/j.bpj.2010.11.044.
24. **Neidhardt FC, Bloch PL, Smith DF.** 1974. Culture medium for enterobacteria. J. Bacteriol. **119:**736–747.
25. **Culham DE, Henderson J, Crane RA, Wood JM.** 2003. Osmosensor ProP of *Escherichia coli* responds to the concentration, chemistry and molecular size of osmolytes in the proteoliposome lumen. Biochemistry **42:**410–420. http://dx.doi.org/10.1021/bi0264364.
26. **Boos W, Ehmann U, Forkl H, Klein W, Rimmele M, Postma P.** 1990. Trehalose transport and metabolism in *Escherichia coli*. J. Bacteriol. **172:**3450–3461.
27. **Smith PK, Krohn RI, Hermanson GT, Mallia AK, Gartner FH, Provenzano MD, Fujimoto EK, Goeke NM, Olson BJ, Klenk DC.** 1985. Measurement of protein using bicinchoninic acid. Anal. Biochem. **150:**76–85.
28. **Romantsov T, Helbig S, Culham DE, Gill C, Stalker L, Wood JM.** 2007. Cardiolipin promotes polar localization of osmosensory transporter ProP in *Escherichia coli*. Mol. Microbiol. **64:**1455–1465. http://dx.doi.org/10.1111/j.1365-2958.2007.05727.x.
29. **Kuru E, Hughes HV, Brown PJ, Hall E, Tekkam S, Cava F, De Pedro MA, Brun YV, VanNieuwenhze MS.** 2012. In situ probing of newly synthesized peptidoglycan in live bacteria with fluorescent D-amino acids. Angew. Chem. Int. Ed. Engl. **51:**12519–12523. http://dx.doi.org/10.1002/anie.201206749.
30. **Laemmli UK.** 1970. Cleavage of structural proteins during the assembly of the head of bacteriophage T4. Nature **227:**680–685.
31. **Schagger H, von Jagow G.** 1987. Tricine-sodium dodecyl sulfate-polyacrylamide gel electrophoresis for the separation of proteins in the range from 1 to 100 kDa. Anal. Biochem. **166:**368–379.
32. **Smith MN, Crane RA, Keates RAB, Wood JM.** 2004. Overexpression, purification and characterization of ProQ, a post-translational regulator for osmoregulatory transporter ProP of *Escherichia coli*. Biochem. **43:**12979–12989. http://dx.doi.org/10.1021/bi048561g.
33. **Weski J, Ehrmann M.** 2012. Genetic analysis of 15 protein folding factors and proteases of the *Escherichia coli* cell envelope. J. Bacteriol. **194:**3225–3233. http://dx.doi.org/10.1128/JB.00221-12.
34. **Cowles CE, Li Y, Semmelhack MF, Cristea IM, Silhavy TJ.** 2011. The free and bound forms of Lpp occupy distinct subcellular locations in *Escherichia coli*. Mol. Microbiol. **79:**1168–1181. http://dx.doi.org/10.1111/j.1365-2958.2011.07539.x.
35. **Hiemstra H, Nanninga N, Woldringh CL, Inouye M, Witholt B.** 1987. Distribution of newly synthesized lipoprotein over the outer membrane and the peptidoglycan sacculus of an *Escherichia coli lac-lpp* strain. J. Bacteriol. **169:**5434–5444.
36. **Suzuki H, Nishimura Y, Yasuda S, Nishimura A, Yamada M, Hirota Y.** 1978. Murein-lipoprotein of *Escherichia coli*: a protein involved in the stabilization of bacterial cell envelope. Mol. Gen. Genet. **167:**1–9.
37. **Margolin W.** 2009. Sculpting the bacterial cell. Curr. Biol. **19:**R812–R822. http://dx.doi.org/10.1016/j.cub.2009.06.033.
38. **Typas A, Banzhaf M, Gross CA, Vollmer W.** 2012. From the regulation

of peptidoglycan synthesis to bacterial growth and morphology. Nat. Rev. Microbiol. **10:**123–136. http://dx.doi.org/10.1038/nrmicro2677.
39. **Iwai N, Nagai K, Wachi M.** 2002. Novel S-benzylisothiourea compound that induces spherical cells in *Escherichia coli* probably by acting on a rod-shape-determining protein(s) other than penicillin-binding protein 2. Biosci. Biotechnol. Biochem. **66:**2658–2662. http://dx.doi.org/10.1271/bbb.66.2658.
40. **Gitai Z, Dye NA, Reisenauer A, Wachi M, Shapiro L.** 2005. MreB actin-mediated segregation of a specific region of a bacterial chromosome. Cell **120:**329–341. http://dx.doi.org/10.1016/j.cell.2005.01.007.
41. **Sykes RB, Bonner DP, Bush K, Georgopapadakou NH.** 1982. Azthreonam (SQ 26,776), a synthetic monobactam specifically active against aerobic gram-negative bacteria. Antimicrob. Agents Chemother. **21:**85–92.
42. **Curtis NA, Eisenstadt RL, Turner KA, White AJ.** 1985. Inhibition of penicillin-binding protein 3 of *Escherichia coli* K-12. Effects upon growth, viability and outer membrane barrier function. J. Antimicrob. Chemother. **16:**287–296.
43. **Singh SK, SaiSree L, Amrutha RN, Reddy M.** 2012. Three redundant murein endopeptidases catalyse an essential cleavage step in peptidoglycan synthesis of Escherichia coli K12. Mol. Microbiol. **86:**1036–1051. http://dx.doi.org/10.1111/mmi.12058.
44. **Hara H, Abe N, Nakakouji M, Nishimura Y, Horiuchi K.** 1996. Overproduction of penicillin-binding protein 7 suppresses thermosensitive growth defect at low osmolarity due to an *spr* mutation of *Escherichia coli*. Microb. Drug Resist. **2:**63–72.
45. **Stalmach ME, Grothe S, Wood JM.** 1983. Two proline porters in *Escherichia coli* K-12. J. Bacteriol. **156:**481–486.
46. **Milner JL, Wood JM.** 1989. Insertion *proQ220*::Tn*5* alters regulation of proline porter II, a transporter of proline and glycine betaine in *Escherichia coli*. J. Bacteriol. **171:**947–951.
47. **Smith MN, Kwok SC, Hodges RS, Wood JM.** 2007. Structural and functional analysis of ProQ: an osmoregulatory protein of *Escherichia coli*. Biochemistry **46:**3084–3095. http://dx.doi.org/10.1021/bi6023786.
48. **Kempf B, Bremer E.** 1998. Uptake and synthesis of compatible solutes as microbial stress responses to high osmolality environments. Arch. Microbiol. **170:**319–330.
49. **Smith-Frieday MN.** 2009. Ph.D. thesis. University of Guelph, Guelph, Ontario, Canada.
50. **Dinnbier U, Limpinsel E, Schmid R, Bakker EP.** 1988. Transient accumulation of potassium glutamate and its replacement by trehalose during adaptation of growing cells of *Escherichia coli* K-12 to elevated sodium chloride concentrations. Arch. Microbiol. **150:**348–357.
51. **Wood JM.** 2011. Bacterial osmoregulation: a paradigm for the study of cellular homeostasis. Annu. Rev. Microbiol. **65:**215–238. http://dx.doi.org/10.1146/annurev-micro-090110-102815.
52. **Cayley S, Lewis BA, Guttman HJ, Record MT, Jr.** 1991. Characterization of the cytoplasm of *Escherichia coli* K-12 as a function of external osmolarity: implications for protein-DNA interactions *in vivo*. J. Mol. Biol. **222:**281–300.
53. **Cayley S, Lewis BA, Record MT, Jr.** 1992. Origins of the osmoprotective properties of betaine and proline in *Escherichia coli* K-12. J. Bacteriol. **174:**1586–1595.
54. **Cayley S, Record MT, Jr.** 2003. Roles of cytoplasmic osmolytes, water and crowding in the response of *Escherichia coli* to osmotic stress: basis of osmoprotection by glycine betaine. Biochemistry **42:**12596–12609. http://dx.doi.org/10.1021/bi0347297.
55. **van Biesen T, Frost LS.** 1994. The FinO protein of IncF plasmids binds FinP antisense RNA and its target, traJ mRNA, and promotes duplex formation. Mol. Microbiol. **14:**427–436.
56. **Jerome LJ, van Biesen T, Frost LS.** 1999. Degradation of FinP antisense RNA from F-like plasmids: the RNA-binding protein, FinO, protects FinP from ribonuclease E. J. Mol. Biol. **285:**1457–1473.
57. **Jerome LJ, Frost LS.** 1999. *In vitro* analysis of the interaction between the FinO protein and FinP antisense RNA of F-like conjugative plasmids. J. Biol. Chem. **274:**10356–10362.
58. **Valentin-Hansen P, Eriksen M, Udesen C.** 2004. The bacterial Sm-like protein Hfq: a key player in RNA transactions. Mol. Microbiol. **51:**1525–1533. http://dx.doi.org/10.1111/j.1365-2958.2003.03935.x.
59. **Keiler KC, Sauer RT.** 1996. Sequence determinants of C-terminal substrate recognition by the Tsp protease. J. Biol. Chem. **271:**2589–2593.
60. **Huerta AM, Collado-Vides J.** 2003. $\sigma^{70}$ promoters in *Escherichia coli*: specific transcription in dense regions of overlapping promoter-like signals. J. Mol. Biol. **333:**261–278. http://dx.doi.org/10.1016/j.jmb.2003.07.017.
61. **Cho BK, Zengler K, Qiu Y, Park YS, Knight EM, Barrett CL, Gao Y, Palsson BO.** 2009. The transcription unit architecture of the *Escherichia coli* genome. Nat. Biotechnol. **27:**1043–1049. http://dx.doi.org/10.1038/nbt.1582.
62. **Silber KR, Sauer RT.** 1994. Deletion of the *prc* (*tsp*) gene provides evidence for additional tail-specific proteolytic activity in *Escherichia coli* K-12. Mol. Gen. Genet. **242:**237–240.
63. **Tadokoro A, Hayashi H, Kishimoto T, Makino Y, Fujisaki S, Nishimura Y.** 2004. Interaction of the *Escherichia coli* lipoprotein NlpI with periplasmic Prc (Tsp) protease. J. Biochem. **135:**185–191. http://dx.doi.org/10.1093/jb/mvh022.
64. **Weiss DS.** 2004. Bacterial cell division and the septal ring. Mol. Microbiol. **54:**588–597. http://dx.doi.org/10.1111/j.1365-2958.2004.04283.x.
65. **Aramini JM, Rossi P, Huang YJ, Zhao L, Jiang M, Maglaqui M, Xiao R, Locke J, Nair R, Rost B, Acton TB, Inouye M, Montelione GT.** 2008. Solution NMR structure of the NlpC/P60 domain of lipoprotein Spr from *Escherichia coli*: structural evidence for a novel cysteine peptidase catalytic triad. Biochemistry **47:**9715–9717. http://dx.doi.org/10.1021/bi8010779.
66. **Weski J, Meltzer M, Spaan L, Mcnig T, Oeljeklaus J, Hauske P, Vouilleme L, Volkmer R, Boisguerin P, Boyd D, Huber R, Kaiser M, Ehrmann M.** 2012. Chemical biology approaches reveal conserved features of a C-terminal processing PDZ protease. ChemBioChem **13:**402–408. http://dx.doi.org/10.1002/cbic.201100643.
67. **Tsatskis Y, Khambati J, Dobson M, Bogdanov M, Dowhan W, Wood JM.** 2005. The osmotic activation of transporter ProP is tuned by both its C-terminal coiled-coil and osmotically induced changes in phospholipid composition. J. Biol. Chem. **280:**41387–41394. http://dx.doi.org/10.1074/jbc.M508362200.
68. **Romantsov T, Stalker L, Culham DE, Wood JM.** 2008. Cardiolipin controls the osmotic stress response and the subcellular location of transporter ProP in *Escherichia coli*. J. Biol. Chem. **283:**12314–12323. http://dx.doi.org/10.1074/jbc.M109871200.
69. **Romantsov T, Battle AR, Hendel JM, Martinac B, Wood JM.** 2009. Protein localization in *Escherichia coli* cells: comparison of cytoplasmic membrane proteins ProP, LacY, ProW, AqpZ, MscS, and MscL. J. Bacteriol. **192:**912–924. http://dx.doi.org/10.1128/JB.00967-09.
70. **Guyer MS, Reed RR, Steitz JA, Low KB.** 1981. Identification of a sex-factor-affinity site in *E. coli* as gamma delta. Cold Spring Harbor Symp. Quant. Biol. **45:**135–140.
71. **Wood JM.** 1981. Genetics of L-proline utilization in *Escherichia coli*. J. Bacteriol. **146:**895–901.
72. **Cormack BP, Valdivia RH, Falkow S.** 1996. FACS-optimized mutants of the green fluorescent protein (GFP). Gene **173:**33–38.
73. **Newton WA, Beckwith JR, Zipser D, Brenner S.** 1965. Nonsense mutants and polarity in the *lac* operon of *Escherichia coli*. J. Mol. Biol. **14:**290–296.
74. **Zipser D, Zabell S, Rothman J, Grodzicker T, Wenk M.** 1970. Fine structure of the gradient of polarity in the z gene of the *lac* operon of *Escherichia coli*. J. Mol. Biol. **49:**251–254.
75. **Lin Z, Johnson LC, Weissbach H, Brot N, Lively MO, Lowther WT.** 2007. Free methionine-(R)-sulfoxide reductase from *Escherichia coli* reveals a new GAF domain function. Proc. Natl. Acad. Sci. U. S. A. **104:**9597–9602. http://dx.doi.org/10.1073/pnas.0703774104.
76. **Kornitzer D, Teff D, Altuvia S, Oppenheim AB.** 1991. Isolation, characterization, and sequence of an *Escherichia coli* heat shock gene, *htpX*. J. Bacteriol. **173:**2944–2953.